Effect of Ni concentration on quantum-well states of the alloy system $Ag/Fe_{1-x}Ni_x$: A spin- and angle-resolved photoemission study

I.-G. Baek,[1] W. Kim,[2] E. Vescovo,[1] and Hangil Lee[1,3,*]

[1]*National Synchrotron Light Source, Brookhaven National Laboratory, Upton, New York 11973, USA*

[2]*Advanced Industrial Technology Group, Division of Advanced Technology, Korea Research Institute of Standards and Science, Daejeon 305-600, Korea*

[3]*Beamline Research Division, Pohang Accelerator Laboratory (PAL), Pohang University of Science and Technology, Pohang 790-784, Republic of Korea*

(Received 3 April 2006; revised manuscript received 23 May 2006; published 5 September 2006)

We investigate the quantum-well states (QWSs) of Ag on an Fe-Ni alloy film grown on a W(110) substrate, using spin- and angle-resolved photoemission spectroscopy (SPARPES). As the Ni content is increased, the Fe-Ni alloy undergoes a transition from a bcc (110) structure to a fcc (111) structure at a Ni concentration of 30%. In the bcc (110) region, we found that as the Ni concentration was increased, the binding energy shifted linearly toward higher binding energy in the QWSs of a thin Ag film, with a maximum shift of 0.4 eV for a Ni concentration of 30%. Our SPARPES data and phase accumulation model calculation indicate that this shift is due to electron doping resulting from inserting Ni, which has two more electrons than Fe. In the fcc (111) region, by contrast, the binding energy shift in the QWSs is barely noticeable, indicating that the potential shift caused by electron doping is insufficiently large in this region. Moreover, as the Ni concentration is increased, a decrease in the polarization of QWSs is observed, which can be attributed to the reduced exchange splitting energy.

DOI: 10.1103/PhysRevB.74.113302 PACS number(s): 73.63.Hs, 75.20.En, 75.50.Bb, 75.70.−i

I. INTRODUCTION

The physical property of low-dimensional systems has been one of the major interests of modern physicists as well as material scientists because it can be well described with the basic quantum picture and has many applications in the material science field. Since the observation of the quantum size effect in a thin film was reported,[1] intense research has been done on semiconductors into its potential applications to electronic devices.[2–4] A quantum well (QW) is an electronic state reflected and confined by potential walls. The conditions for formation of quantum-well states (QWSs) directly depend on the reflectivity at the interface. Therefore, perfect reflectivity is acquired when the interface is perfectly smooth and a band gap exists in each reflector material so that the electron wave function in the spacer cannot penetrate across the interface. In addition, QW-like structure (a QW resonance) can be enhanced without a band gap in the case of different symmetry between the spacer material and the reflector material, or interface roughness.[5–7]

The QWSs in metal films only began to receive significant research interest after it was discovered that magnetic coupling between two ferromagnetic films separated by a nonmagnetic spacer could give rise to the giant magnetoresistance effect.[8,9] This magnetic coupling has been found to oscillate between parallel and antiparallel coupling depending on the thickness of the spacer materials.[10–12] The period of this oscillation can be modulated by use of alloys instead of pure metals[13] or by changing the orientation[14] of the spacer materials. However, to date no attempt has been made to modulate the binding energy of the QWSs in these systems. In research on semiconductors, by contrast, various attempts have been made to modulate QWSs by changing the doping conditions or applying an electric or magnetic field.[15] In a manner analogous to the doping of semiconductor quantum walls, the QWSs confined in metallic thin films can be modulated by using alloy films as the wall materials.

Here, we report a spin- and angle-resolved photoemission spectroscopy (SPARPES) study on Ag QWSs confined by an $Fe_{1-x}Ni_x$ alloy film epitaxially grown on the W(110) surface. The binding energy shift and the spin polarization of the QWSs are taken over the whole range from pure Fe to pure Ni ($0.0 \leq x \leq 1.0$). Moreover, the phase accumulation model calculation has been obtained to understand the correlation between the binding energy shift and the electronic structure of the ferromagnetic material as the potential wall.

II. EXPERIMENT

The experiments were performed at the U5UA undulator beamline at the National Synchrotron Light Source of the Brookhaven National Laboratory.[16] The SPARPES data were collected using a 50 mm hemispherical analyzer coupled with a low-energy diffuse scattering spin polarimeter. The total energy resolution was about 100 meV and the angular resolution was about 2°. The base pressure was 5×10^{-11} torr. Fe and Ni were coevaporated onto the W(110) surface using a dual *e*-beam evaporator at 400 K. The total pressure was kept below 1.5×10^{-10} torr during film deposition. Sharp low-energy electron diffraction (LEED) patterns were acquired for all binary alloy compositions, ensuring epitaxial growth of the film. The deposition rate was calibrated with a quartz crystal monitor. The thickness of the alloy films was maintained at 12–15 Å for all compositions. In the case of the thicker films, on the other hand, the LEED patterns showed less sharp intensities, which indicated that the roughness of the films is increased. Ag was evaporated on the alloy film by thermal evaporation at liquid nitrogen

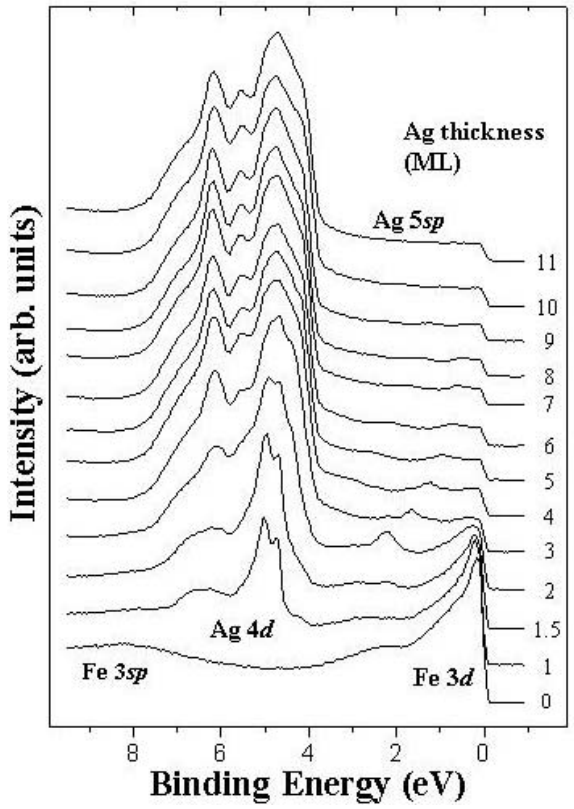

FIG. 1. The valence band photoemission spectra of Ag on Fe(110) film as a function of Ag thickness (from 0.0 to 11.0 ML) taken at 40 eV with normal emission.

(LN_2) temperature and postannealed at room temperature to avoid island growth. All QWS data were also collected at LN_2 temperature. The spin-resolved measurements were performed in magnetic remanence. A magnetization pulse was applied in the in-plane direction between the [001] and $[1\bar{1}0]$ crystallographic directions of W(110) to magnetize the sample. The two orthogonal in-plane components of the polarization vector were measured simultaneously by our spin detector.[17] All spectra were taken at normal emission with a photon energy of $h\nu$=40 eV.

III. RESULTS AND DISCUSSION

Figure 1 shows the valence band spectra for Ag confined between an Fe(110) film and a vacuum as a function of Ag thickness expressed in terms of Ag(111) monolayers (MLs). Inspection of the Ag 5*sp* state region of the spectra clearly reveals that discrete QWSs emerge and disappear in this region as the Ag thickness is varied. By contrast, the shape of the feature corresponding to the Ag 4*d* state changes only a small amount although the Ag thickness is increased above 4.0 ML. Moreover, we found that Ag 4*d* QWSs are only observed when the thickness is less than 4.0 ML whereas Ag 5*sp* QWSs are observed up to 11.0 ML. It can be explained by the fact that the *d* electron is more localized than the *sp* electron. Interestingly, these QWSs are spin polarized in the minority state as the QWSs of Ag 5*sp* character are

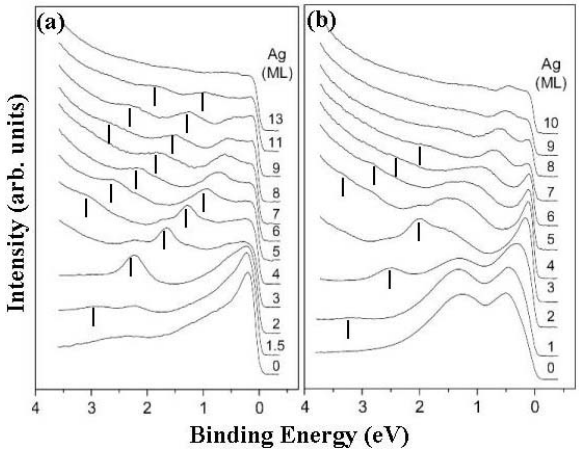

FIG. 2. The photoemission spectra of the QWSs (marked with |) and resonances of Ag 5*sp* band on (a) Fe(110) and (b) Ni(111) film grown on W(110) substrate as a function of Ag thickness.

produced in the region where only the Fe 3*d* minority spin band has a hybridization gap. This will be discussed further below in relation to the Fe-Ni alloy case.

Figure 2 shows the Ag 5*sp* QWSs on the Fe(110) and Ni(111) surfaces in detail. In both sets of spectra, we can observe discrete QWSs up to 10.0 ML. Based on the LEED pattern investigated in our experiment and the previous studies of the Ag/Fe(110) systems,[18,19] the Ag films on the $Fe_{1-x}Ni_x$(110) surface are expected to grow epitaxially or show a layer-by-layer-like growth mode. As the thickness of the Ag layer is increased, the QWSs are evolving toward the Ag valence band maximum located around 0.3 eV along the Ag(111) direction. These QWSs in Ag(111) thin films have already been well studied in Ag/Cu(111),[5] Ag/Au(111),[20] Ag/W(110),[21] and Ag/V(100) (Ref. 22) systems; these previous studies found similar QW evolution to the bulk band edge.

We also performed a phase accumulation model calculation for the Ag 5*sp* QWSs confined by either an Fe(110) or a Ni(111) interface and compared the results with the experimental data. We adopted the formalism presented in Ref. 23 for QWSs confined in a band gap, modifying it to add a scattering phase shift term (Φ_{scatt}) to the original phase accumulation model for the partially confined QW resonance states from different symmetry bands.[21] Thus, the quantization condition becomes

$$\Phi_C + \Phi_B + m2ka - \Phi_{scatt} = 2\pi n, \tag{1}$$

where Φ_C and Φ_B are the phase shifts upon reflection at the interface and the vacuum level, respectively, and m, k, and a denote the number of overlayers, the wave vector of propagation, and the thickness of one monolayer, respectively. The solution is graphically acquired from the crossing points of the $m2ka$ curves and $2\pi n - \Phi_C - \Phi_B + \Phi_{scatt}$ curves, as shown in Fig. 3. In addition, our experimental data are projected on the curve of the phase accumulation, $m2ka$. We assume that scattered phase shift for a specific binding energy in the resonance region is in proportion to the k value of the Fe Σ_5^2

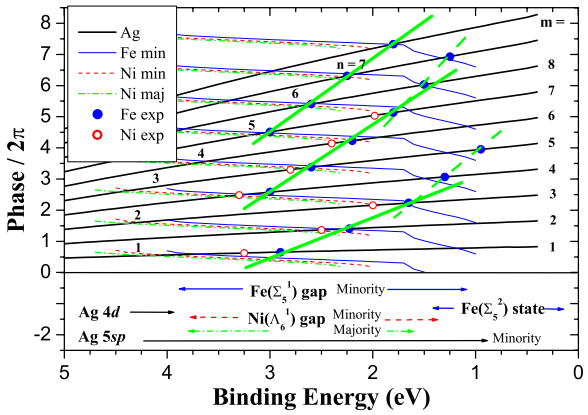

FIG. 3. (Color online) The phase energy diagram for the Ag overlayer on Fe(110) and Ni(111). Thick solid curves represent the QW phase accumulation $m2ka$ with layer number m. Thin solid, dashed, and dotted curves, respectively, represent the phase change $2\pi n - \Phi_C - \Phi_B$ from Fe minority, Ni minority, and Ni majority gap with node number n. Filled circles and empty circles are the experimental binding energies of the QWSs on Fe(110) and Ni(111), respectively, projected on the Ag 5sp band. The crossing points of the thick solid curves and the other curves are where the QWSs are enhanced. As shown with green thick line, we can clearly see a different trend between resonance and nonresonance states. Hence, we apply the extended model only in the resonance region.

minority state of corresponding binding energy. Under this assumption, we can reproduce the binding energies of quantum well resonance states. As shown in Fig. 3, the calculation successfully reproduces the binding energies of the QWSs except for the 1.0 ML case. It is well known that the simplified phase accumulation model is not applicable to the single-monolayer case. In this calculation, only the minority spin bands of Fe are taken into account because the majority spin band has no gap in the region of the QWSs. Between binding energies of 1.0 and 1.7 eV in the Fe Σ_5^1 band gap, the additional scattering phase shift is included because the Fe Σ_5^2 band is overlapped in this energy region.

On the other hand, both majority and minority bands are taken into account for Ni because the exchange energy of Ni ($\Delta_{ex,\mathrm{Ni}} \simeq 0.3$ eV) is much smaller than that of Fe ($\Delta_{ex,\mathrm{Fe}} \simeq 2.0$ eV), such that both Ni spin bands have a gap in this energy region. Therefore, we can confidently predict that the QWSs in the Fe case will be much more spin polarized than those in the Ni case; as will be seen below, the spin-resolved spectra indicate that this prediction is correct. As mentioned above, QW resonance can exist outside the band gap. Above binding energy 1.0 eV in Fig. 2(a) and 2.0 eV in Fig. 2(b), QW resonances are observed that have broader and less intense peaks than QWSs. It is noted that our calculation reproduces the experimental QWS binding energy, even though the Fe(110) surface and the Ag(111) overlayer have different symmetries. This can be understood by considering the Ag Λ band as a linear combination of Fe Σ bands. Since the binding energies of the QWSs on Ni and Fe with the same Ag thickness differ by about 0.4 eV, a continuous shift in binding energy is expected when the potential well is modified continuously by alloying Fe with Ni.

We prepared Fe-Ni alloy films with various compositions as an interfacial layer for a Ag spacer in order to clarify the

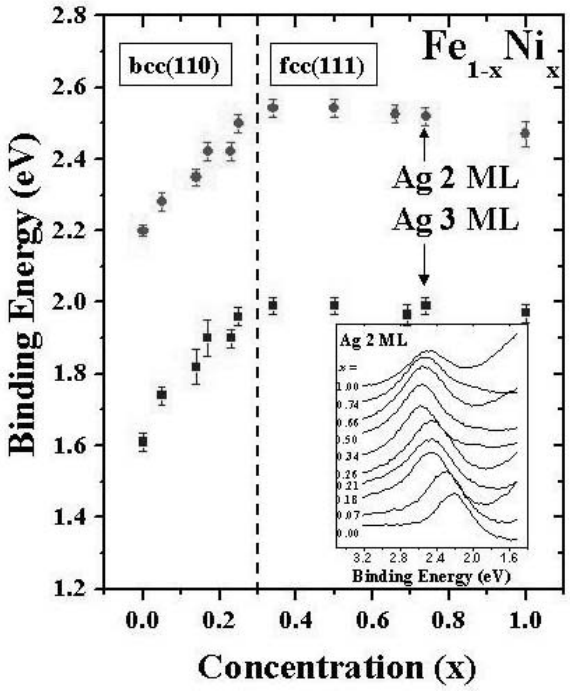

FIG. 4. The binding energy of the QWSs when Ag thickness is 2.0 and 3.0 ML as a function of Ni composition. Inset is raw data of the Ag 2 ML QWSs with various alloy compositions.

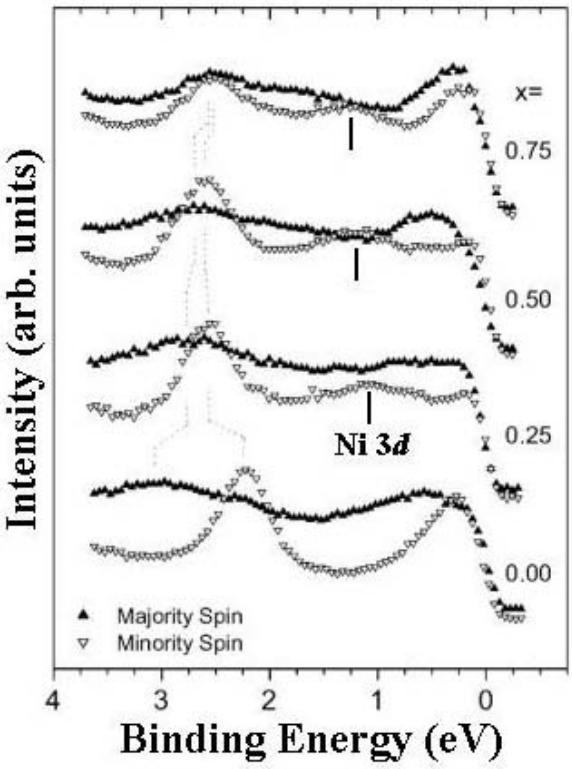

FIG. 5. The spin-resolved photoemission spectra of Ag 2.0 ML QWSs taken at $h\nu$=40 eV with normal emission for various alloy compositions x=0, 0.25, 0.5, 0.75. Ni 3d states are marked with |. The binding energy change with the QWS (resonance) in minority (majority) spin state is indicated with dotted line.

effect of an alloy film as a spacer. In our previous study, we found that as the Ni concentration was increased up to 30%, a sharp transition was observed in the integrated valence band photoemission spectra, where the Fe-like *sp* state switches to the Ni-like *sp* state and satellite.[24] Figure 4 shows that as Ni is gradually mixed into the pure Fe, the binding energy of the Ag QWSs shifts linearly toward higher energy until the Ni content becomes 30%. As the Ni content is further increased, however, the binding energy appears to move slightly toward lower binding energy. The linear binding energy shift in the Fe-rich region can be understood as an electron doping effect. As Ni has two more electrons than Fe, the electron doping caused by adding Ni into a Fe site pushes the energy levels higher, thereby making the potential well deeper. As a result, the QWSs shift to higher binding energy by an amount equal to the potential well shift. At a Ni concentration of 30%, however, a structural transition takes place and the electron doping picture breaks down. Specifically, the band gap position for Ni concentrations above 30% becomes similar to that of pure Ni.

To clarify the change of both the majority and minority spin bands separately, we recorded the spin-resolved photoemission spectra for the QWSs. Figure 5 shows each spin state of the QW for a Ag thickness of 2.0 ML and different alloy compositions. The QWS becomes less polarized as x increases, which can be attributed to the fact that Fe has a higher magnetic moment than Ni. Moreover, the decrease in the exchange energy from Fe to Ni causes the sharp minority spin QWS and the broad majority spin QW resonance to come closer and look similar, as indicated by the dotted line. Hence, both the minority spin QWS and the majority spin QW resonance undergo the biggest shifts between $x=0$ and 0.25. The shift in the minority spin state occurs because the marked Ni $3d$ (Λ_6^1) state in the minority spin state appears at 1.2 eV, pulling down the upper edge of the minority band gap. At the same time, the band gap in the majority spin state is supposed to be pushed up by the Ni state.

IV. CONCLUSION

Discrete Ag QWSs in a $Ag/Fe_{1-x}Ni_x$ alloy system were successfully produced and studied over the full range of binary alloy composition. As Ni was added to pure Fe, a linear shift in the binding energy was observed up to $x=0.3$. In the SPARPES spectra, we observed sharp QW states in the minority spin band, and broad QW resonances in the majority spin band. As Fe is alloyed with Ni, the spin polarization and the binding energy difference between the minority QWS and the majority QW resonance decreased due to the reduced exchange energy. These results can be well understood using the phase accumulation model.

ACKNOWLEDGMENT

This work was supported by Grant No. R01-2006-000-11247-0 from the Basic Research Program of the Korea Science and Engineering Foundation.

*Electronic address: easyscan@postech.ac.kr

[1] M. Jalochowski, M. Hoffmann, and E. Bauer, Phys. Rev. B **51**, 7231 (1995).
[2] P. Czoschke, Hawoong Hong, L. Basile, and T.-C. Chiang, Phys. Rev. B **72**, 075402 (2005).
[3] L. Gavioli, K. R. Kimberlin, M. C. Tringides, J. F. Wendelken, and Z. Zhang, Phys. Rev. Lett. **82**, 129 (1999).
[4] W. B. Su, H. Y. Lin, Y. P. Chiu, H. T. Shih, T. Y. Fu, Y. W. Chen, C. S. Chang, and Tien T. Tsong, Phys. Rev. B **71**, 073304 (2005).
[5] M. A. Mueller, T. Miller, and T.-C. Chiang, Phys. Rev. B **41**, 5214 (1990).
[6] T. Miller, A. Samsavar, and T.-C. Chiang, Phys. Rev. B **50**, 17686 (1994).
[7] T.-C. Chiang, Surf. Sci. Rep. **39**, 181 (2000).
[8] M. N. Baibich, J. M. Broto, A. Fert, F. Nguyen Van Dau, F. Petroff, P. Etienne, G. Creuzet, A. Friedrich, and J. Chazelas, Phys. Rev. B **61**, R2472 (2000).
[9] F. J. Himpsel, J. E. Ortega, G. J. Mankey, and R. F. Willis, Adv. Phys. **47**, 511 (1998).
[10] J. Unguris, R. J. Celotta, and D. T. Pierce, Phys. Rev. Lett. **67**, 140 (1991).
[11] Z. Q. Qiu, J. Pearson, A. Berger, and S. D. Bader, Phys. Rev. Lett. **68**, 1398 (1992).
[12] S. N. Okuno *et al.*, Phys. Rev. Lett. **72**, 764 (1994).
[13] S. S. P. Parkin, C. Chappert, and F. Herman, Europhys. Lett. **24**, 71 (1993).
[14] M. T. Johnson, M. Coehoorn, J. J. de Vries, N. W. E McGee, J. aan de Stegge, and P. J. H. Bloemen, Phys. Rev. Lett. **69**, 969 (1992).
[15] G. Bastard, *Wave Mechanics Applied to Semiconductor Heterostructures* (Edition de Physique, Les Ulis, 1988).
[16] E. Vescovo, H.-J. Kim, Q.-Y. Dong, G. Nintzel, D. Carson, S. L. Hulbert, and N. V. Smith, Synchrotron Radiat. News **12**, 10 (1999).
[17] J. Unguris, D. T. Pierce, and R. J. Celotta, Rev. Sci. Instrum. **57**, 1314 (1986).
[18] Z. Q. Qiu, J. Pearson, and S. D. Bader, Phys. Rev. B **45**, 7211 (1992).
[19] T. Furukawa and K. Koike, Phys. Rev. B **57**, 2694 (1998).
[20] T. Miller, A. Samsavar, G. E. Franklin, and T.-C. Chiang, Phys. Rev. Lett. **61**, 1404 (1988).
[21] A. M. Shikin, D. V. Vyalikh, G. V. Prudnikova, and V. K. Adamchuk, Surf. Sci. **487**, 135 (2001).
[22] D. P. Woodruff, M. Milun, and P. Pervan, J. Phys.: Condens. Matter **11**, L105 (1999).
[23] N. V. Smith, N. B. Brookes, Y. Chang, and P. D. Johnson, Phys. Rev. B **49**, 332 (1994).
[24] Hangil Lee, I.-G. Baek, S. Kim, and E. Vescovo, Surf. Sci. (to be published).